Elsevier Editorial System(tm) for Journal of Environmental Radioactivity
Manuscript Draft

Manuscript Number:

Title: Investigation of temperature and barometric pressure variation effects on radon concentration in the Sopronbánfalva Geodynamic Observatory, Hungary

Article Type: Research Paper

Keywords: Radon concentration; Air pressure; Temperature; Underground gallery; Data analysis.

Corresponding Author: Prof. Gyula Mentes, DSc

Corresponding Author's Institution: Research Centre for Astronomy and Earth Sciences, Hungarian Academy of Sciences, Geodetic and Geophysical Institute

First Author: Gyula Mentes, DSc

Order of Authors: Gyula Mentes, DSc; Ildikó Eper-Pápai

Abstract: Radon concentration variation has been monitored since 2009 in the artificial gallery of the Sopronbánfalva Geodynamic Observatory, Hungary. In the observatory, the radon concentration is extremely high, 100 - 600 kBq m-3 in summer and some kBq m-3 in winter. The relationships between radon concentration, temperature and barometric pressure were separately investigated in the summer and winter months by Fast Fourier Transform, Principal Component Analysis, Multivariable Regression and Partial Least Square analyses in different frequency bands. It was revealed that the long-period radon concentration variation is mainly governed by the temperature (20 kBq m-1 °C-1) both in summer and winter. The regression coefficients between long-period radon concentration and barometric pressure are -1.5 KBq m-3 hPa-1 in the summer and 5 KBq m-3 hPa-1 in the winter months. In the 0.072-0.48 cpd frequency band the effect of the temperature is about -1 kBq m-3 °C-1 and that of the barometric pressure is -5 KBq m-3 hPa-1 in summer and -0.5 KBq m-3 hPa-1 in winter. In the high frequency range (> 0.48 cpd) all regression coefficients are one order of magnitude smaller than in the range of 0.072-0.48 cpd. Fast Fourier Transform of the radon concentration, temperature and barometric pressure time series revealed S1, K1, P1, S2, K2, M2 tidal constituents in the data and week O1 components in the radon concentration and barometric pressure series. A detailed tidal analysis, however, showed that the radon tidal components are not directly driven by the gravitational force but rather by solar radiation and barometric tide. Principal Component Analysis of the raw data was performed to investigate the yearly, summer and winter variability of the radon concentration, temperature and barometric pressure. In the summer and winter periods the variability does not change. The higher variability of the radon concentration compared to the variability of the temperature and the barometric pressure shows that besides the temperature and barometric pressure variations other agents, e.g. natural ventilation of the observatory, wind, etc. also play an important role in the radon concentration variation.

Investigation of temperature and barometric pressure variation effects on radon concentration in the Sopronbánfalva Geodynamic Observatory, Hungary

Gyula Mentes*, Ildikó Eper-Pápai

Geodetic and Geophysical Institute, Research Centre for Astronomy and Earth Sciences, Hungarian Academy of Sciences, Csatkai E. u. 6-8., H-9400 Sopron, Hungary

*Corresponding author. Tel: +36-99-508348, Fax: +36-99-508-355

E-mail: mentes@ggki.hu

Ildikó Eper-Pápai: E-mail: papai@ggki.hu

Tel: +36-99-508348, Fax: +36-99-508-368

Highlights

Causes of Rn concentration variations are investigated in different frequency ranges.
Long-period temperature variation has the largest effect on Rn concentration.
Barometric pressure causes mainly short-periodic Rn concentration variations.
Tidal frequencies in Rn concentration do not directly caused by gravity tide.

Investigation of temperature and barometric pressure variation effects on radon concentration in the Sopronbánfalva Geodynamic Observatory, Hungary

Abstract

Radon concentration variation has been monitored since 2009 in the artificial gallery of the Sopronbánfalva Geodynamic Observatory, Hungary. In the observatory, the radon concentration is extremely high, 100 – 600 kBq m^{-3} in summer and some kBq m^{-3} in winter. The relationships between radon concentration, temperature and barometric pressure were separately investigated in the summer and winter months by Fast Fourier Transform, Principal Component Analysis, Multivariable Regression and Partial Least Square analyses in different frequency bands. It was revealed that the long-period radon concentration variation is mainly governed by the temperature (20 kBq m^{-1} °C^{-1}) both in summer and winter. The regression coefficients between long-period radon concentration and barometric pressure are –1.5 KBq m^{-3} hPa^{-1} in the summer and 5 KBq m^{-3} hPa^{-1} in the winter months. In the 0.072-0.48 cpd frequency band the effect of the temperature is about –1 kBq m^{-3} °C^{-1} and that of the barometric pressure is –5 KBq m^{-3} hPa^{-1} in summer and –0.5 KBq m^{-3} hPa^{-1} in winter. In the high frequency range (> 0.48 cpd) all regression coefficients are one order of magnitude smaller than in the range of 0.072-0.48 cpd. Fast Fourier Transform of the radon concentration, temperature and barometric pressure time series revealed S1, K1, P1, S2, K2, M2 tidal constituents in the data and week O1 components in the radon concentration and barometric pressure series. A detailed tidal analysis, however, showed that the radon tidal components are not directly driven by the gravitational force but rather by solar radiation and barometric tide. Principal Component Analysis of the raw data was performed to investigate the yearly, summer and winter variability of the radon concentration, temperature and

barometric pressure. In the summer and winter periods the variability does not change. The higher variability of the radon concentration compared to the variability of the temperature and the barometric pressure shows that besides the temperature and barometric pressure variations other agents, e.g. natural ventilation of the observatory, wind, etc. also play an important role in the radon concentration variation.

Keywords: Radon concentration; Air pressure; Temperature; Underground gallery; Data analysis

1. Introduction

Radon (^{222}Rn) is an inert, omnipresent radioactive gas, one of the daughter elements of ^{238}U and its direct mother element is ^{226}Ra. ^{238}U and ^{226}Ra occur at varying concentration in the Earth crust and in soils derived from different rock types. Radon gas, which is continuously produced in rocks and soils, migrates into the air. The migration is mainly affected by convection and molecular diffusion (Steinitz and Piatibratova, 2010; Szabó et al., 2013). Thus, the amount of radon emanation depends on the elastic properties and porosity of the rocks and on the local fracture system (e.g. Holub and Brady, 1981; Kies et al., 2002, 2005; Vaupotič et al., 2010) and shows large temporal variations due to meteorological and hydrological effects (Garavaglia et al. 1999; Vargas and Ortega, 2006; Papp et al., 2008; Smetanova et al., 2010; Steinitz and Piatibratova, 2010; Szabó et al., 2013). Analysis of temporal variations in the radon gas concentration is a useful tool to study geodynamic processes associated with tectonic (Garavaglia et al., 1998, 2000; Aumento, 2002; Omori et al., 2007; Mahajan et al., 2010; Utkin and Yurkov, 2010) and volcanic (Toutain and Baubron, 1999; Viñas et al., 2007) activities as well as in looking for a warning sign for earthquakes (Igarashi et al., 1995; Yong and Wei, 1995; Garavaglia et al., 1999; Virk et al., 2000; Crockett et al., 2006; Kawada et al., 2007; Inan et al., 2008; Yasuoka et al., 2009; Crockett and Gillmore, 2010; Cigoliní et al., 2015). For this reason the relationship between rock strain and radon concentration is an important scientific issue to be answered. Holub and Brady (1981) investigated the connection between radon emanation and rock stress in laboratory. Trique et al. (1999) and Kies at al. (2002, 2005) conducted measurements in tunnels near water reservoirs seeking for the correspondence between radon concentration and rock strain due to loading and unloading effect of the reservoir. Garavaglia et al. (2000) found low correlation between tilt-strain and radon emission in underground observatories. Several papers deal with the connection of radon concentration and Earth tides (Alekseenko et al., 2010) in underground caves (Barnet et al., 1997a, 1997b; Kies et al., 1999) and in dwellings (Groves-Kirkby et al., 2004). Richon et al. (2009) treat the impact of barometric tides on radon concentration in their publication. Millich et al. (1998) theoretically demonstrated that tidal rock stresses can induce the flow of radon bearing pore fluid. Barnet et al. (1997a; 1997b) graphically compared radon data series of several days with the theoretical tidal components. Other publications demonstrate that the amount of radon emanation strongly depends on the temperature and air pressure (Barnet et al., 1997a, 1997b; Gregorič et al., 2011; Pinault and Baubron, 1996; William and Wilkening, 1974). The problem is worsened by the fact that both temperature and air pressure have an indirect effect, as their changes induce stress in the rock. According to the complexity of the radon emanation process and the influence of environmental effects, the interpretation of radon concentration variation as a possible proxy of small scale geodynamic processes and deformations is not yet resolved unambiguously. The understanding of seasonal and weather-related variations of radon concentration is essential for planning mitigation schemes and for studying the relationship between rock strain and radon concentration variations accurately. The object of this study is to investigate the relations of indoor radon concentration to barometric pressure and temperature variations on the basis of five year long data series measured in the artificial underground gallery of the Sopronbánfalva Geodynamic Observatory (SGO) in years from 2009 till 2013. The results of this study provide a quantitative description of the relationships in short and long period time domains.

2. Observation site

The Sopronbánfalva Geodynamic Observatory is located on the Hungarian-Austrian border in the Sopron Mountains. The area belongs to the extensions of the Eastern Alps represented by crystalline rocks and is characterized by their outcrops in this Lower Alps (Alpokalja) region (Fig. 1.a). The Sopron Mountains are made of metamorphic rocks from the Palaeozoic age such as gneiss and different mica schists (Kisházi and Ivancsics, 1985; Fülöp, 1990; Haas, 2001). The geological map of the surroundings of the observatory is shown in Fig. 1c. The coordinates of the observatory (SGO in Fig. 1) are: latitude 47º40’55’’ N; longitude 16º33’32” E; the altitude is 280 m a.s.l. The observatory is an artificial gallery at a depth of about 60 m driven horizontally into an outcrop of the bedrock formed by gneiss. The ground plan of the observatory and the location of the AlphaGUARD^{TM} radon concentration measuring instrument in the gallery are delineated in Fig. 1b. The instrument is placed near to an extensometer about 40 m from the entrance and it is thermally insulated by three doors but not perfectly hermetically sealed. It means that there is a slow air circulation via the conduit for the electric cables of the instruments. This ventilation does not change the temperature in the gallery but it ensures that the indoor and outdoor barometric pressures are the same. Thus we can safely assume that the transport of radon to the outside is very slow. The yearly mean temperature in the gallery is 10.4 ºC and the yearly and daily temperature variations are less than 0.5 ºC and 0.05 ºC, respectively. The relative humidity is 90% and it is nearly constant. There is no human activity in the observatory. The instruments are remote-controlled via the Internet from the institute, so anthropogenic effects can be excluded.

3. Methods

3.1. Measuring method

The radon concentration has been measured by a radon monitor type AlphaGUARD^{TM} (PQ2000PRO). The AlphaGUARD^{TM} is able to continuously determine the radon concentration as well as to record air pressure, temperature and humidity (http://www.genitron.de, last access 14.08.2014). The instrument incorporates a pulse-counting ionization chamber (using alpha spectroscopy). This radon monitor is suitable for continuous monitoring of radon concentration between 2 Bq m^{-3} and 2 MBq m^{-3}. Its sensitivity is 5 cpm at 100 Bq m^{-3} and it has a stable long-term calibration factor. The measurements are carried out in diffusion mode.

In addition to the radon concentration, the inner and outer temperature and barometric pressure were also measured hourly. Radon concentration, outer temperature and outer air pressure data were subjected to data processing, as the inner temperature was constant (10.4 ºC) and the inner and outer barometric pressures did not differ significantly.

3.2. Data processing

In addition to analysing raw data, the measured data (radon concentration, temperature and barometric pressure) were analysed in different frequency ranges. Adjacent averaging (4800 adjacent data involved in the averaging), band-pass filter with cut-off frequencies of 0.072–0.48 cpd (~2–14 days), high-pass filter (with cut-off frequency of 0.48 cpd) and daily averaging were used to study the variations in different frequency ranges. Raw data, adjacent-averaged and filtered data were subjected to Principal Component Analysis (PCA), Multivariable Regression (MVR) and Partial Least Square (PLS) analyses (Abdi, 2003). Fast Fourier Transform (FFT) of the data series was performed for comparing the spectral components of the signals. Data processing was carried out by the ORIGIN 9.1 program (http://www.originlab.com, last access 11.08.2014). The relationships between radon concentration, barometric pressure and temperature were also separately investigated in the summer (from 1 May to 30 September) and winter periods (from 1 November to 31 March). ETERNA 3.4 program package (Wenzel, 1996) was used for the calculation of the theoretical tidal potential and tidal evaluation of data.

4. Results and discussion

Figure 2 shows the hourly measured radon concentration, outdoor temperature and barometric pressure data from 1 January 2009 till 31 December 2013. At first glance, it is conspicuous that the radon concentrations in the summer and winter periods are quite unlike. The radon concentration is quickly increasing when the outer temperature exceeds the temperature (10.4 °C) inside the observatory. The summer months are characterized by extremely high concentration (100 – 600 kBq m^{-3}). In the winter months, both the mean value and the variability of the radon concentration drop to some kBq m^{-3} (see also Garavaglia et al., 1998; Przylibski, 1999; Martin-Luis et al., 2002; Perrier et al., 2007; Gregorič et al., 2011; Loisy and Cerepi, 2012; Fijałkowska-Lichwa, 2014).

Figure 3 shows the amplitude spectra of the measured raw data. The relationship between the amplitudes of radon concentration and meteorological parameters shows a great variability (see e.g. Steinitz and Piatibratova, 2010). To get a better insight into the connection between these quantities, Pearson (usual linear correlation) and Spearman correlation, as well as linear regression analysis were carried out. Results are summarized in Table 1. The small value of the Spearman correlation coefficients show that the radon concentration changes are not monotonous in the function of the changes of barometric pressure and temperature, namely the increasing values of the meteorological parameters “accidentally” cause decreasing radon concentration values and conversely (Steinitz and Piatibratova, 2010).

In Fig. 4 radon concentration amplitudes are plotted against temperature (a) and barometric pressure (b), moreover regression lines are determined between these quantities. The regression coefficients are given in Table 1. The obtained radon concentration patterns confirm the results concluded from the Spearman correlation.

In the amplitude spectrum clear diurnal and semi-diurnal tidal components (Melchior, 1978; Wilhelm et al., 1997) are present but a ter-diurnal component is absent as it was also found by Pinault and Baurbon (1996) in contrast with Steinitz and Piatibratova (2010) who recorded a ter-diurnal component. In Fig. 5 the assumed tidal components are denoted in the amplitude spectrum in the diurnal (a) and semi-diurnal (b) tidal frequency ranges. In the diurnal frequency band the S1 (1.000 cpd) solar radiation and K1 (1.002925 cpd) luni-solar components are clearly present in the radon concentration. P1 (0.997091815 cpd) principal solar and the O1 ((0.929512006 cpd) principal lunar components can also be detected, but the presence of these components is questionable due to their small amplitudes relative to the neighbouring components. K1 and P1 frequencies represent the annual modulation of S1 (Boyarsky et al., 2003) which explains their presence in the radon concentration. In the semi-diurnal band the presence of the S2 (2.000 cpd) principal solar and the K2 (2.005012531 cpd) luni-solar components is evident and the M2 (1.932367 cpd) principal lunar component appears with small amplitude. The S1 and S2 solar tidal components are present in our data similarly to other published results (e.g. Kies et al., 1999; Groves-Kirkby et al., 2006; Alekseenko et al., 2010; Steinitz and Piatibratova 2010). To determine the origin of the tidal constituents in the radon concentration data, the tidal components of the theoretical tidal potential, , calculated for the location of the SGO, and the measured radon concentration data series were adjusted by means of the ETERNA 3.4 program package. The results in Fig. 6 demonstrate that the ratios of the radon concentration components to the theoretical tidal potential constituents are very different. Quite unlike ratios for the main tidal waves O1 (0.115) and M2 (0.004) indicate clearly that the tidal components in the radon concentration are not of direct gravitational origin at the location of the SGO. Probably they are governed by the air pressure variations caused by atmospheric tide, weather variations and solar radiation. Similarly, Steinitz and Piatibratova (2010) did not reveal the principal lunar waves O1 and M2 besides the S1, S2 and S3 components. In contrast with these results, Lenzen and Neugebauer (1999) detected the mentioned components in an abandoned gypsum mine, presumably owing to the different measurement site. Richon et al. (2012) also detected the M2 and O1 waves in a subglacial laboratory. Crockett et al. (2010) investigated the tidal effect at two measurement sites. At one location they found the weak presence of the M2 wave, while at the other location the wave was not detected and in consequence they assumed that the detected S1 and S2 waves are due to the effects of temperature and air pressure. Friederich and Wilhelm (1985) investigated the solar radiation effects on Earth tide measurements. Similarly to us, they found that the solar radiation effect is considerable in the S1, K1 diurnal frequencies while this effect is diminished by a factor of ten in the semidiurnal S2, K2 frequencies, so it can be neglected. At the SGO S2 is diminished by a factor of six and K2 by a factor of two. In the radon concentration the S1 amplitude is high but within the theoretical tidal potential waves this component is the smallest. It also supports the observation that tidal components of directly gravitational origin cannot be detected in our radon concentration data.

PCA analysis of the raw data was performed to investigate the yearly, summer (from 1 of May to 30 of September of the actual year) and winter (from 1 of November of the actual year to 31 March of the next year) variability of radon concentration, temperature and barometric pressure. The results are summarised in Table 2. The variability of the three parameters is the same in the summer and winter periods while from the yearly data series it is about 10 percent higher in the case of radon concentration and about 50 percent less in the case of temperature than summer and winter values. The variability of barometric pressure is about the same for all the periods. From the higher variability of radon concentration compared to the variability of temperature and barometric pressure it can be concluded that there should also be other agents governing the radon concentration variation besides temperature and air pressure. Such agents could be the ventilation (e.g. Perrier et al., 2004, 2005, 2007; Eff-Darwich et al., 2008; Akbari et al., 2013; Finkelstein et al., 2006), wind (Riley et al., 1996), rain (Garavaglia et al., 1998; Dal Moro et al., 2000, Perrier et al., 2007), ground water variations (e.g. Pinault and Baubron, 1996; Smetanová, 2010), etc.

To get numerical relations between radon concentration, barometric pressure and temperature variation in different frequency bands, the data series were filtered by a high-pass (cut off frequency: 0.48 cpd) and a band-pass filter (low cut off frequency: 0.072 cpd and high cut off frequency: 0.48 cpd) furthermore the daily averages were calculated to eliminate daily variations. Figure 7, as an example, shows the diverse patterns of the high-pass and band-pass filtered data. In Fig 7a the high-pass filtered data in the summer month July of 2009 (above) and in the winter month December of 2009 (below) are plotted. In Fig.7b the band-pass filtered data in the summer months from 1 June to 31 August of 2009 (above) and in the winter months from 1 November of 2009 to 31 January of 2010 (below) are plotted. In the high-pass filtered radon concentration a two-day period while in the band-pass-filtered data a two-week period can be observed (see e.g. Steinitz and Piatibratova, 2010; Szabó et al., 2013). Such kind of obvious periodicity is present neither in the summer radon concentration data nor in the temperature and barometric pressure data of summer and winter periods.

To study the long-period behaviour of radon concentration, the data were filtered by an adjacent filter. The average values were calculated from 4800 adjacent data points which corresponds to an average of 200-day data (a cut off frequency of 0.005 cpd). Figure 8 shows the long-period variation. From the Figure it is obvious that the radon concentration is mainly governed by temperature in the long-period range.

Since the MVR and PLS analyses methods have different algorithm, the raw and filtered data were subjected to both analysis. In each year the data were treated separately in the winter and summer months similarly to the PCA analysis. The year by year parameters from the summer and winter months were separately averaged for every data types (raw, filtered, and averaged data). The results of the two analysis methods were practically identical, therefore only the results of the PLS analysis are listed in Table 3. In the summer months the regression coefficient between radon and temperature is positive and varies between 16 and 25 kBq m^{-3} $°C^{-1}$ in the case of raw, daily and adjacent averaged data. It is negative in the case of the band-pass and high-pass filtered data and its value is one order of magnitude smaller in the 0.072-0.48 cpd frequency range (band-pass) than the value obtained in the case of raw and averaged (daily and adjacent) data. In the high frequency range (greater than 0.48 cpd) the regression coefficient is –0.233 kBq m^{-3} $°C^{-1}$. Since the long-period components of radon concentration appear both in the raw and averaged data, we can assume that they are mainly governed by temperature in the summer months. In the short-period band the effect of temperature is much smaller, and has an opposite effect, than in the long-period band. In the summer months the regression coefficients have a value in the same order and they are negative except in the high-pass filtered frequency range. In the winter months when the outer temperature is lower than the inner temperature, the regression coefficients between radon concentration and temperature are about one order of magnitude smaller than in the summer months in the case of the raw, daily averaged, band- and high-pass filtered data, while the regression coefficients between radon concentration and barometric pressure are about the quarter of the values obtained for the summer months. It means that the radon concentration is mainly governed by the barometric pressure in the winter months. In the long-period range (adjacent averaged data) the regression coefficient between radon concentration and temperature is the same as in the summer months. The regression coefficient between radon concentration and barometric pressure is positive and about five times higher than in the summer months. This positive effect of the temperature and air pressure (increasing temperature and barometric pressure causes increasing radon concentration) can be seen very well in Fig. 8. The strainmeter in the observatory measures a seasonal strain variation depending on the temperature. This temperature effect is described by Mentes (2000) in detail. In Figure 8 the long-period, seasonal strain variation is not plotted because it’s course is similar to the temperature curve. The observatory is sensitive to air pressure variations due to the atmospheric loading on the rock at the observatory and in its surroundings (Gebauer et al., 2010; Eper-Pápai et al., 2014). It can be inferred that the long-period radon concentration is governed by the rock temperature due to thermal expansion of the pores, interstices, cracks of the rock (e.g. Weinlich et al. 2006; Kawada et al., 2007; Vaupotič et al., 2010) and by the long-term atmospheric loading (Holub and Brady, 1981), especially by weather fronts deforming the rock and pressing the radon into the air (e.g. William and Wilkening, 1974; Crockett et al., 2006). This effect can be observed in Fig. 8. When the barometric pressure is high, the radon concentration values are also increasing even if the temperature is unchanged.

6. Conclusions

The five-year simultaneous data record reveals a complex relationship between, temperature, air pressure and radon concentration data. The most apparent characteristic of the radon emanation potential at the measurement site is its quite different behaviour in the winter and summer. In the summer months the concentration is between 100 and 600 kBq m^{-3}, while in the winter months the radon concentration drops to some kBq m^{-3}. Natural ventilation due to the temperature variation is mainly responsible for this high concentration differences. The amplitude spectrum of radon concentration, temperature and barometric time series revealed S1, K1, P1, S2, K2, M2 tidal constituents in the data series and a week O1 component. The tidal analysis of radon concentration yielded practically the same tidal components. The amplitude ratios of radon and theoretical tidal components are very different, from which it can be inferred that the radon tidal components are not directly driven by the gravitational force but by the solar radiation and barometric tides.

PCA analysis of the raw data was performed to investigate the yearly, summer and winter variability of radon concentration, temperature and barometric pressure. In the summer and winter periods the variability does not change. From the higher variability of radon concentration than the variability of temperature and barometric pressure it can be concluded that there should also be other agents (e.g. natural ventilation of the observatory) governing the radon concentration variation besides the temperature and air pressure.

Different behaviour of the radon concentration variation in the summer and winter months was investigated also by PLS analysis. Results revealed that the dependence of the radon concentration on temperature and barometric pressure is different in the different frequency ranges. In the long-period range, when the frequency is smaller than 0.072 cpd, the effect of the temperature is about the same in the summer and winter months (about 20 kBq m^{-3} $°C^{-1}$). The regression coefficients between radon concentration and barometric pressure are –1.5 KBq m^{-3} hPa^{-1} in the summer and 5 KBq m^{-3} hPa^{-1} in the winter months. While the effect of the temperature is always positive, barometric pressure has a negative effect in summer and a positive effect in winter (increasing barometric pressure causes increasing radon concentration). In the 0.072-0.48 cpd frequency range, the effect of the temperature is about –1 kBq m^{-3} $°C^{-1}$ and the effect of barometric pressure is –5 KBq m^{-3} hPa^{-1} in summer and –0.5 KBq m^{-3} hPa^{-1} in winter. In the high frequency range (> 0.48 cpd) all regression coefficients are one order of magnitude smaller than in the range of 0.072-0.48 cpd. In this frequency range the temperature has a positive effect in summer.

Acknowledgements

This work was funded by the Hungarian National Research Fund (OTKA) under the project No. K 71952 and K 109060. Special thanks are given to Tibor Molnár for his careful maintenance of the instruments.

References

Abdi, H., 2003. PLS-Regression; Multivariate analysis. In: Lewis-Beck, M., Bryman, A., Futing, T., (Eds): Encyclopedia for research methods for the social sciences. Thousand Oaks (CA): Sage.

Akbari, K., Mahmoudi, J., Ghanbari, M., 2013. Influence of indoor air conditions on radon concentration in a detached house. J. Environ. Radioactiv. 116, 166–173. http://dx.doi.org/10.1016/j.jenvrad.2012.08.013.

Alekseenko, V.V., Gavriluk, M.Yu., Kuzminov, V.V., Stenkin, V.Yu., 2010. Tidal effect in the radon-due neutron flux from the Earth’s crust. J. Phys. Conf. Ser. 203, 012045. doi:10.1088/1742-6596/203/1/012045.

Aumento, F., 2002. Radon tides on an active volcanic island: Terceira, Azores. Geofis. Int., 41 (4), 499–505.

Barnet, I., Kies, A., Skalský, L., Procházka, J., 1997a. Radon variations and Earth tides in the unventilated underground spaces. Bull. Chech. Geol. Surv. 72 (2), 105–114.

Barnet, I., Procházka, J., Skalský, L., 1997b. Do the Earth tides have an influence on short-term variations in radon concentration? Radiat. Prot. Dosim. 69 (1), 51–60.

Boyarsky, E.A., Ducarme, B., Latynina, L.A., Vandercoilden, L., 2003. An attempt to observe the Earth liquid core resonance with extensometers at Protvino Observatory. Bull. d’Inf. Marées Terr. 138, 10987–11009.

Cigolini C., Laiolo M., Coppola. D., 2015. The LVD signals during the early-mid stages of the L'Aquila seismic sequence and the radon signature of some aftershocks of moderate magnitude. J. Environ. Radioactiv. 139, 56–65. http://dx.doi.org/10.1016/j.jenvrad.2014.09.017.

Crockett, R.G.M., Gillmore, G.K., Phillips, P.S., Denman, A.R., Groves-Kirkby, C.J., 2006. Tidal synchronicity of built-environment radon levels in the UK. Geophys. Res. Lett. 33, L05308. doi:10.1029/2005GL024950.

Crockett, R.G.M., Gillmore, G.K., 2010. Spectral-decomposition techniques for the identification of radon anomalies temporally associated with earthquakes occurring in the UK in 2002 and 2008. Nat. Hazards Earth Sys. Sci. 10, 1079–1084. doi:10.5194/nhess-10-1079-2010.

Dal Moro, G., Garavaglia, M., Zadro, M., 2000. Tilt-Strain Measurements in the NE Italy Seismic Area: Precursor Analysis and Atmospheric Noise Effects. Phys. Chem. Earth (A), 25 (3), 271–276.

Eff-Darwich, A., Viñas, R., Soler, V., de la Nuez, J., Quesada, M.L., 2008. Natural air ventilation in underground galleries as a tool to increase radon sampling volumes for geologic monitoring. Rad. Meas. 43, 1429 – 1436.

Eper-Pápai, I., Mentes, G., Kis, M., Koppán, A., 2014. Comparison of two extensometric stations in Hungary. J. Geodyn. 80, 3–11. http://dx.doi.org/10.1016/j.jog.2014.02.007.

Fijałkowska-Lichwa, L., 2014. Short-term radon activity concentration changes along the Underground Educational Tourist Route in the Old Uranium Mine in Kletno (Sudety Mts., SW Poland). J. Environ. Radioactiv. 135, 25–35.

Finkelstein, M., Eppelbaum, L.V., Price, C., 2006. Analysis of temperature influences on the amplitude–frequency characteristics of Rn gas concentration. J. Environ. Radioactiv. 86, 251–270.

Friederich, W., Wilhelm, H., 1985. Solar radiational effects on Earth tide measurements. In: Ricardo, W. (Ed.), Proc. 10th International Symposium on Earth Tides: with special sessions dedicated to ocean tides. Madrid. pp. 865–880.

Fülöp, J., 1990. Magyarország geológiája. Paleozoikum I. (Geology of Hungary. Palaeozoic I.). Hung. Geol. Inst., Budapest. (in Hungarian)

Garavaglia, M., Braitenberg, C., Zadro, M., 1998. Radon monitoring in a cave of North-Eastern Italy. Phys. Chem. Earth., 23 (9-10), 949–952.

Garavaglia, M., Braitenberg, C., Zadro, M., Quattrochi, F., 1999. Radon measurements in soil and water in the seismic Friuli area. Il Nuovo Cimento C, 22 (3-4), 415–422.

Garavaglia, M., Dal Moro, G., Zadro, M., 2000. Radon and tilt measurements in a seismic area: Temperature effects. Phys. Chem. Earth. (A), 25 (3), 233–237.

Gebauer, A., Steffen, H., Kroner, C., Jahr, T., 2010. Finite element modelling of atmosphere loading effects on strain, tilt and displacement at multi-sensor stations. Geophys. J. Int. 181. 1593–1612, http://dx.doi.org/10.1111/j.1365-246X.2010.04549.x.

Gregorič, A., Zidanšek, A., Vaupotič, J., 2011. Dependence of radon levels in Postojna Cave on outside air temperature. Nat. Hazards Earth Syst. Sci., 11, 1523–1528. doi:10.5194/nhess-11-1523-2011.

Groves-Kirkby, C.J., Denman, A.R., Crockett, R.G.M., Phillips, P.S., 2004. Periodicity in domestic radon time series – evidence for Earth tides. 11th International Congress of the International Radiation Protection Association, Madrid. irpa11.irpa.net/pdfs/6a26.pdf, 1–10.

Groves-Kirkby, C. J., Denman, A.R., Crockett, R.G.M., Phillips, P.S., Gillmore, G.K., 2006. Identification of tidal and climatic influences within domestic radon time-series from Northamptoshire, UK. Sci. Total Environ. 367 (1), 191–202, doi:10.1016/j.scitotenv.2005.11.019.

Haas, J. (Ed.), 2001. Geology of Hungary. Eötvös University Press, Budapest.

Holub, R.F., Brady, B.T., 1981. The effect of Stress on Radon Emanation from Rock. J. Geophys. Res. 86 (B3), 1776–1784.

Igarashi, G., Saeki, S., Takahata, N., Sumikawa, K., Tasaka, S., Sasaki, Y., Takahashi, M., Sano, Y., 1995. Ground-water radon anomaly before the Kobe earthquake in Japan. Science 269, 60–61. doi:10.1126/science.269.5220.60.

Inan , S., Akgul, T., Seyis, C., Saatçilar, R., Baykut, S., Ergintav, S., Baş, M., 2008. Geochemical monitoring in the Marmara region (NW Turkey): A search for precursors of seismic activity. J. Geophys. Res. Solid Earth 113 (3), B03401. doi:10.1029/2007JB005206.

Kawada, Y., Nagahama, H., Omori, Y., Yasuoka, Y., Ishikawa, T., Tokonami, S., Shinogi, M., 2007. Time-scale invariant changes in atmospheric radon concentration and crustal strain prior to a large earthquake. Nonlinear Process. Geophys. 14, 123–130. In: http://www.nonlin-processes-geophys.net/14/123/2007.

Kies, A., Majerus, J., D'Oreye, L., 1999. Underground radon gas concentrations related to Earth tides. Il Nuovo Cimento C, 22(3-4), 287–294.

Kies, A., Massen, F., Tosheva, Z., 2002. Influence of variable stress on underground radon concentrations. Geofis. Int., 41 (3), 325–329.

Kies, A., Massen, F., Tosheva, Z., 2005. Influence of variable stress on underground radon concentrations. Radioact. Environ., 7, 334–329. doi:10.1016/S1569-4860(04)07037-8.

Kisházi, P., Ivancsics, J., 1985. Genetic petrology of the Sopron crystalline schist sequence, Acta Geol. Hun. 28, 191–213.

Lenzen, M., Neugebauer, H.J., 1999. Measurements of radon concentration and the role of Earth tides in a gypsum mine in Walferdange, Luxemburg, Health Physics, 77 (2), 154–162.

Loisy, C., Cerepi, A., 2012. Radon-222 as a tracer of water–air dynamics in the unsaturated zone of a geological carbonate formation: Example of an underground quarry (Oligocene

Aquitain limestone, France). Chem. Geol. 296–297, 39–49. doi:10.1016/j.chemgeo.2011.12.010.

Mahajan, S., Walia, V., Bajwa, B.S., Kumar, A., Singh, S., Seth, N., Dhar, S., Gill, G.S., Yang, T.F., 2010. Soil-gas radon/helium surveys in some neotectonic areas of NW Himalayan foothills, India. Nat. Hazards Earth Syst. Sci. 10, 1221–1227.

Martin-Luis, C., Quesada, M.L., Eff-Darwich, A., De la Nuez, J., Coello, J., Ahijado, A., Casillas, R., Soler, V., 2002. A new strategy to measure radon in an active volcanic island (Tenerife, Canary Islands). Environ. Geol. 43, 72–78.

Melchior, P., 1978. The Tides of the Planet Earth, Pergamon Press, Oxford.

Mentes, G., 2000. Influence of Temperature and Barometric Pressure Variations on Extensometric Deformation Measurements at the Sopron Station, Acta Geod. Geoph. Hung. 35 (3), 277–282.

Millich, E., Neugebauer, H.J., Huenges, E., Nover, G., 1998. Pressure dependence of permeability and earth tide induced fluid flow. Geophys. Res. Lett. 25 (6), 809–812.

Omori, Y., Yasuoka, Y., Nagahama, H., Kawada, Y., Ishikawa, T., Tokonami, S., Shinogi, M., 2007. Anomalous radon emanation linked to preseismic electromagnetic phenomena. Nat. Hazards Earth Syst. Sci. 7, 629–635.

Papp, B., Deák, F., Horváth, Á., Kiss, Á., Rajnai, G., Szabó, Cs., 2008. A new method for the determination of geophysical parameters by radon concentration measurements in bore-hole. J. Environ. Radioactiv. 99, 1731–1735.

Perrier, F., Richon, P., Crouzeix, C., Morrat, P., Le Mouël J.-L., 2004. Radon-222 signatures of natural ventilation regimes in an underground Quarry. J. Environ. Radioactiv. 71, 17–32.

Perrier, F., Richon, P., Sabroux, J.-C., 2005. Modelling the effect of air exchange on ^{222}Rn and its progeny concentration in a tunnel atmosphere. Sci. Total Environ. 350, 136–150.

Perrier, F., Richon, P., Gautam, U., Tiwari, D.R., Shrestha, P., Sapkota, S.N., 2007. Seasonal variations of natural ventilation and radon-222 exhalation in a slightly rising dead-end tunnel. J. Environ. Radioactiv. 97, 220–235.

Pinault, J.-L., Baubron J.-C., 1996. Signal processing of soil gas radon, atmospheric pressure, moisture, and soil temperature data: A new approach for radon concentration modelling. J. Geophys. Res. 101, 3157–3171.

Przylibski, T.A., 1999. Radon concentration changes in the air of two caves in Poland. J. Environ. Radioactiv. 45, 81–94.

Richon, P., Moreau, L., Sabroux, J.-C., Pili, E., Salaün, A., 2012. Evidence of both M_2 and O_1 Earth tide waves in radon-222 air concentration measured in a subglacial laboratory. J. Geophys. Res. 117, B12404. doi:10.1029/2011JB009111.

Richon, P., Perrier, F., Pili, E., Sabroux, J.-C., 2009. Detectability and significance of 12 hr barometric tide in radon-222 signal, dripwater flow rate, air temperature and carbon dioxid concentration in an underground tunnel. Geophys. J. Int. 176, 683–694.

Riley, W.J., Gadgil, A.J., Bonnefocus, Y.C., Nazaroff, W.W., 1996. The effect of steady winds on Radon-222 entry from soil into houses. Atmos. Environ. 30 (7), 1167–1176.

Smetanová, I., Holý, K., Müllerová, M., Polášková, A., Túnyi, I., 2010. Temporal and spatial changes of radon concentration in borehole water (Little Carpathians Mts., Slovakia). Nat. Hazards Earth Syst. Sci. 10, 1373–1377.

Steinitz, G., Piatibratova, O., 2010. Radon signals at the Roded site, Southern Israel, Solid Earth 1, 99–109. doi:10.5194/se-1-99-2010.

Szabó, K.Zs., Jordan, Gy., Horváth, Á., Szabó Cs., 2013. Dynamics of soil gas radon concentration in a highly permeable soil based on a long-term high temporal resolution observation series. J. Environ. Radioactiv. 124, 74–83.

Toutain, J.-P., Baubron, J.-C., 1999. Gas geochemistry and seismotectonics: a review. Tectonophysics 304, 1–27.

Trique, M., Richon, P., Perrier, F., Avouac, J.-P., Sabroux, J.-C., 1999. Radon emanation and electric potential variations associated with transient deformation near reservoir lakes. Nature, 399, 137–141.

Utkin, V.I., Yurkov, A.K., 2010. Radon as a tracer of tectonic movements. Russ. Geol. Geophys. 51 (2), 220–227. doi:10.1016/j.rgg.2009.12.022.

Vargas, A., Ortega, X., 2006. Influence of environmental changes on continuous radon monitors. Results of a Spanish intercomparison exercise. Radiat. Prot. Dosim. 121 (3), 303–309.

Vaupotič, J., Gregorić, A., Kobal, I., Žvab, P., Kozak, K., Mazur, J., Kochowska, E., Grządzdiel, D., 2010. Radon concentration in soil gas and radon exhalation rate at the Ravne Fault in NW Slovenia. Nat. Hazards Earth Syst. Sci. 10, 895–899.

Viñas, R., Eff-Darwich, A., Soler, V., Martín-Luis, M.C., Quesada, M.L., de la Nuez, J., 2007. Processing of radon time series in underground environments: Implications for volcanic surveillance in the island of Tenerife, Canary Islands, Spain. Rad. Meas. 42, 101–115. doi:10.1016/j.radmeas.2006.07.002.

Virk, H.S., Walia, V., Sharma, A.K., Kumar, N., Kumar, R., 2000. Correlation of radon anomalies with microseismic events in Kangara and Chamba valleys of N-W Himalaya. Geofis. Int. 39 (3), 221–227.

Weinlich, F.H., Faber, E., Boušková, A., Josef Horálek, J., Teschner, M., Poggenburg, J., 2006. Seismically induced variations in Mariánské Lázně fault gas composition in the NW Bohemian swarm quake region, Czech Republic — A continuous gas monitoring. Tectonophysics 421, 89–110.

Wenzel, H.G., 1996. The nanogal software: Earth tide data processing package ETERNA 3.30. Bull. d'Inf. Marées Terr. 124, 9425–9439.

Wilhelm, H., Zürn,W., Wenzel, H.G. (Eds.), 1997. Tidal phenomena, Lectures in Earth Sciences. 66, Springer.

William, E.C., Wilkening, M.H., 1974. Atmospheric pressure effects on ^{222}Rn transport across the Earth-air interface, J. Geophys. Res. 79 (33), 5025–5029.

Yasuoka, Y., Kawada, Y., Nagahama, H., Omori, Y., Ishikawa, T., Tokonami, S., Shinogi, M., 2009. Preseismic changes in atmospheric radon concentration and crustal strain, Phys. Chem. Earth 34, 431–434.

Yong, S., Wei, Z., 1995. The correlation between radon variation and Earth solid tide change in rock-groundwater system – the mechanical foundation for using radon change to predict earthquake. J. Earthq. Pred. Res., 4, 423–430.

FIGURE CAPTIONS

Fig. 1. Site of the measurements. a) Location of the Sopronbánfalva Geodynamic Observatory (SGO) in Hungary, b) Ground plan of the SGO, c) Geological map of the surroundings of the SGO (Haas 2001).

Fig. 2. Radon concentration, outdoor barometric pressure and temperature measured between 1 January 2009 and 31 December 2013.

Fig. 3. Fourier amplitude spectra calculated from the data series of air temperature, barometric pressure, and radon concentration. Processed data are from 1 January 2009 till 31 December 2013

Fig. 4. Regression between radon concentration and temperature (a) and barometric pressure (b)

Fig. 5. Fourier amplitude spectra in the diurnal range (a) and in the semidiurnal range (b)

Fig. 6. Theoretical tidal potential calculated for the location of the SGO and tidal constituents calculated from the radon data series

Fig. 7. High-pass (a) and band-pass (b) filtered data in summer (above) and winter (below) months in 2009.

Fig. 8. Long-period relationship between radon concentration, barometric pressure and temperature. Hourly sampled data were filtered by an adjacent average filter using 4800 adjacent data.

Figure 1
Click here to download high resolution image

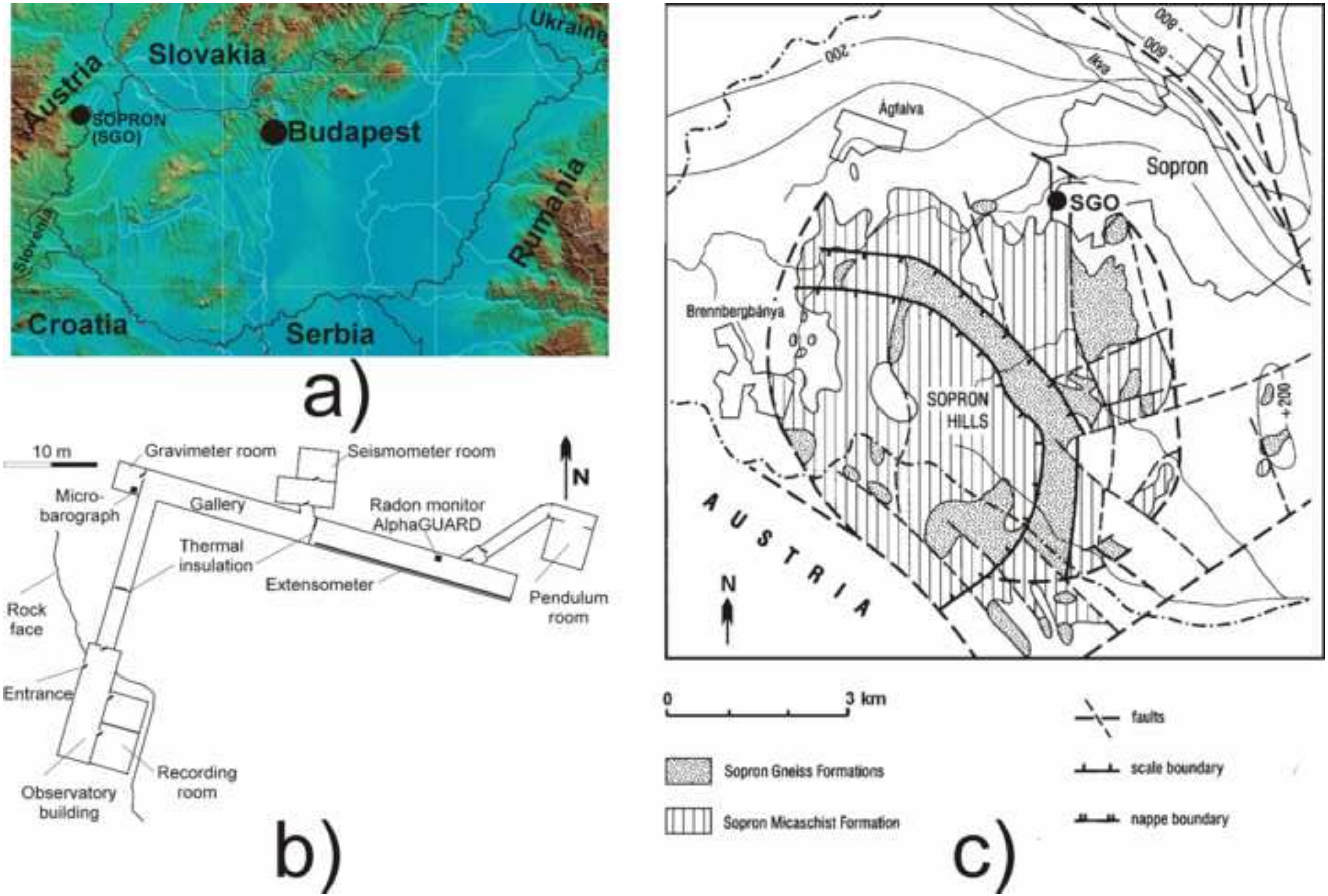

Figure 2

Click here to download high resolution image

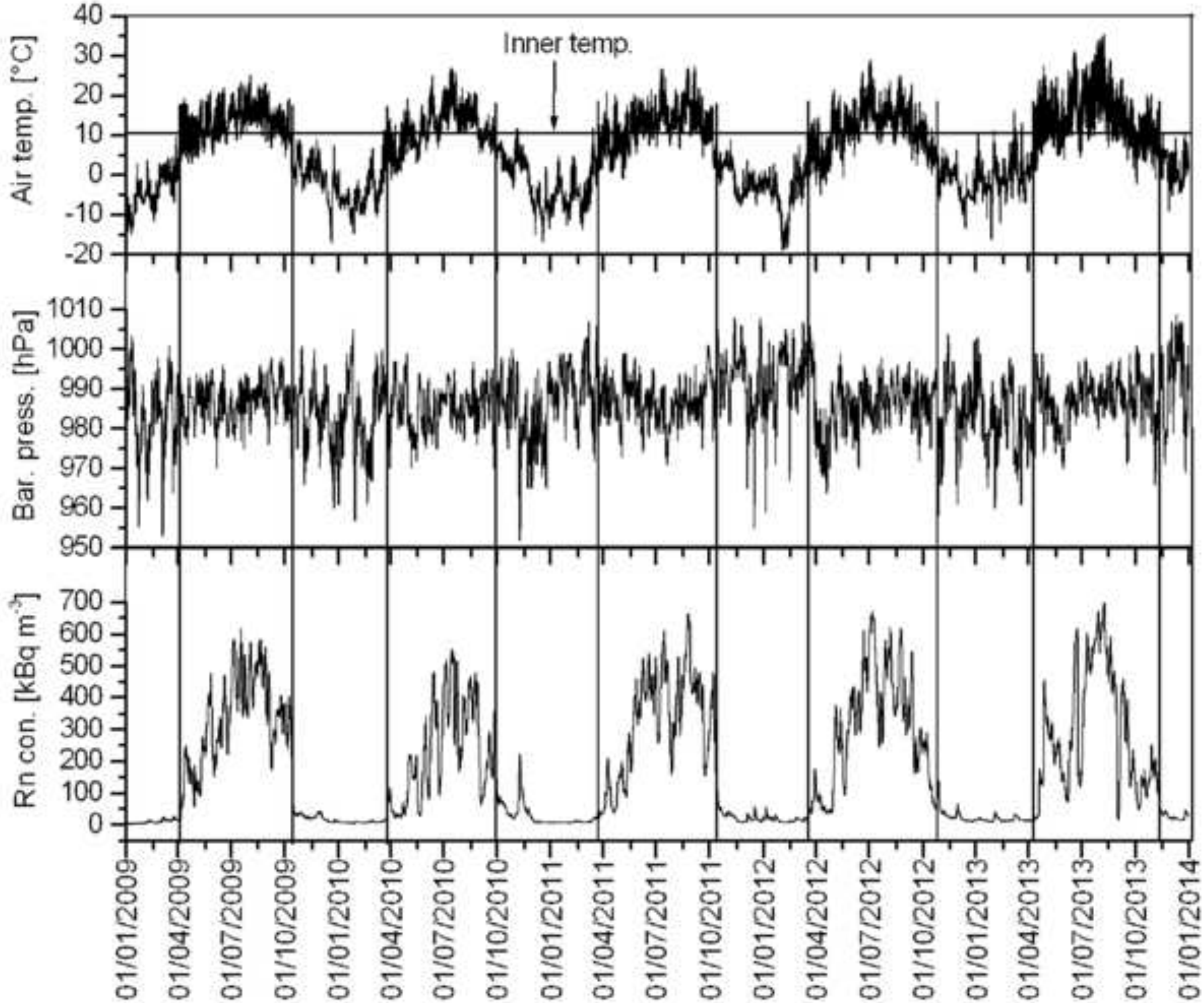

Figure 3
Click here to download high resolution image

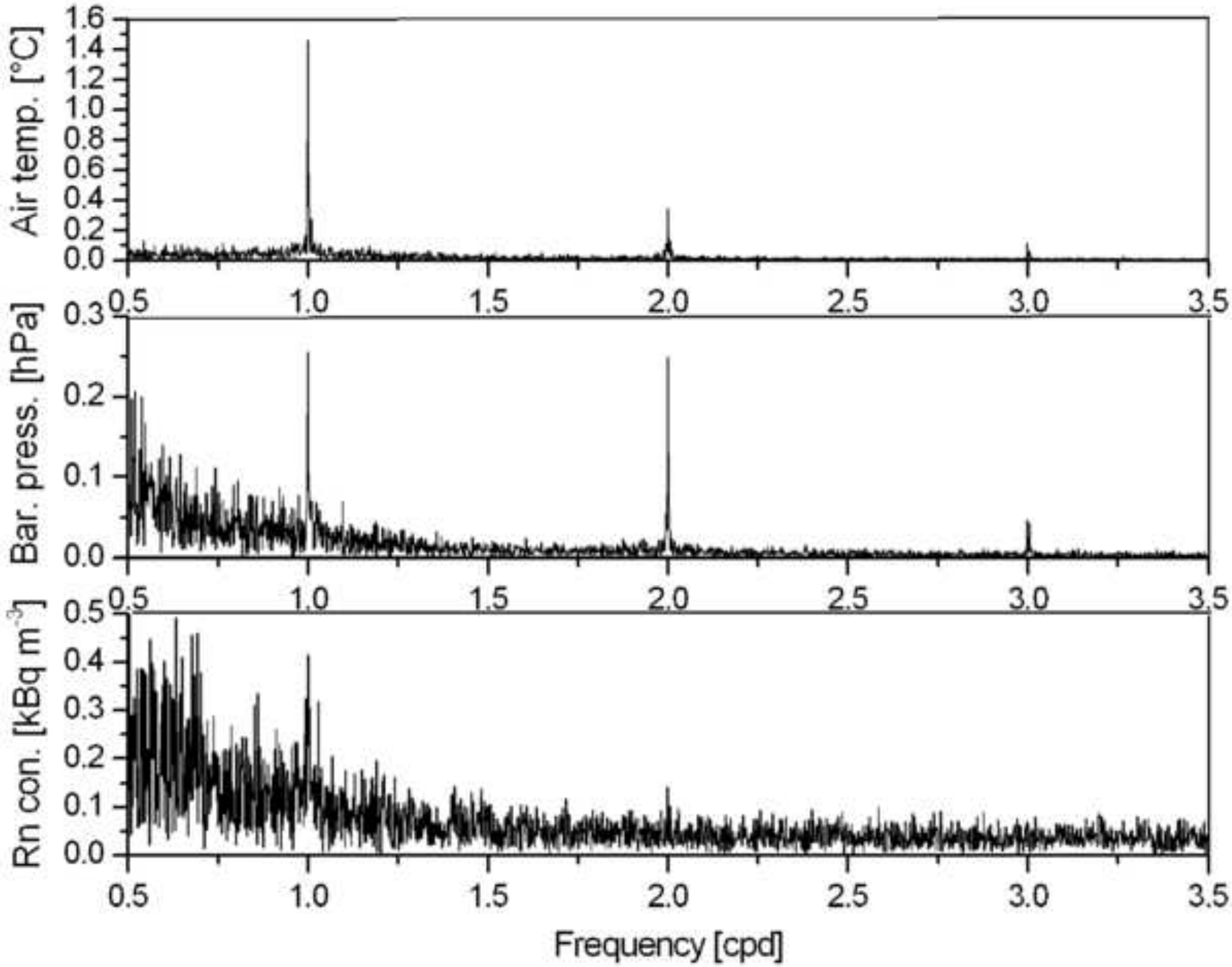

Figure 4

Click here to download high resolution image

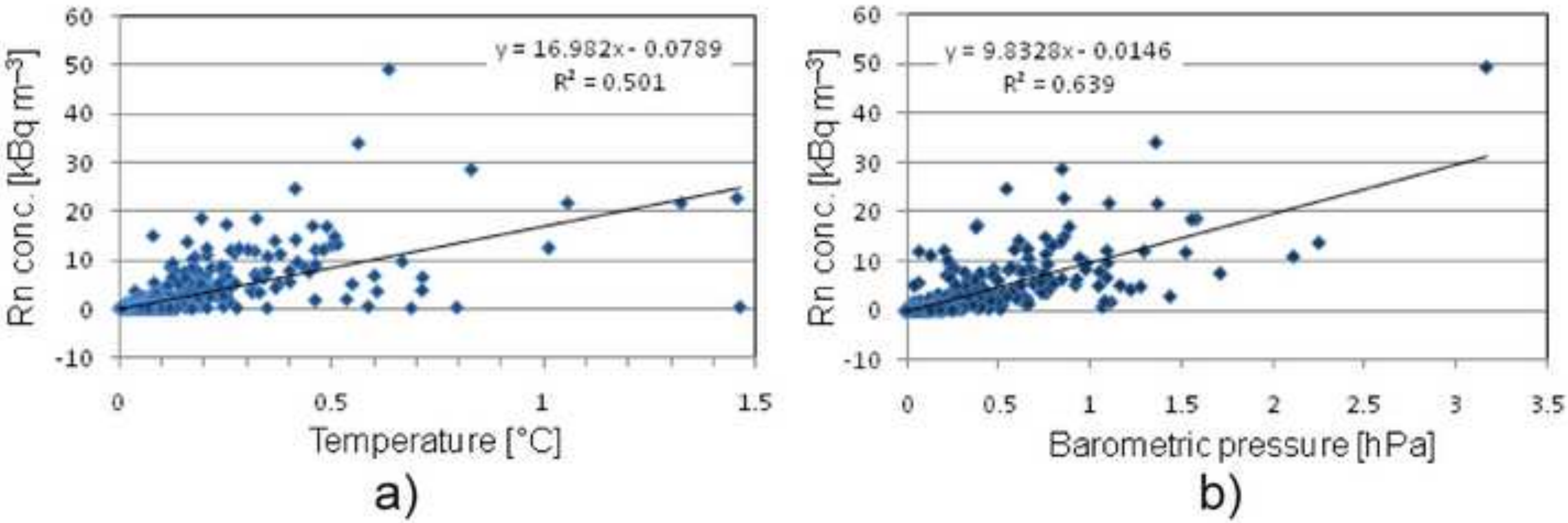

Figure 5
Click here to download high resolution image

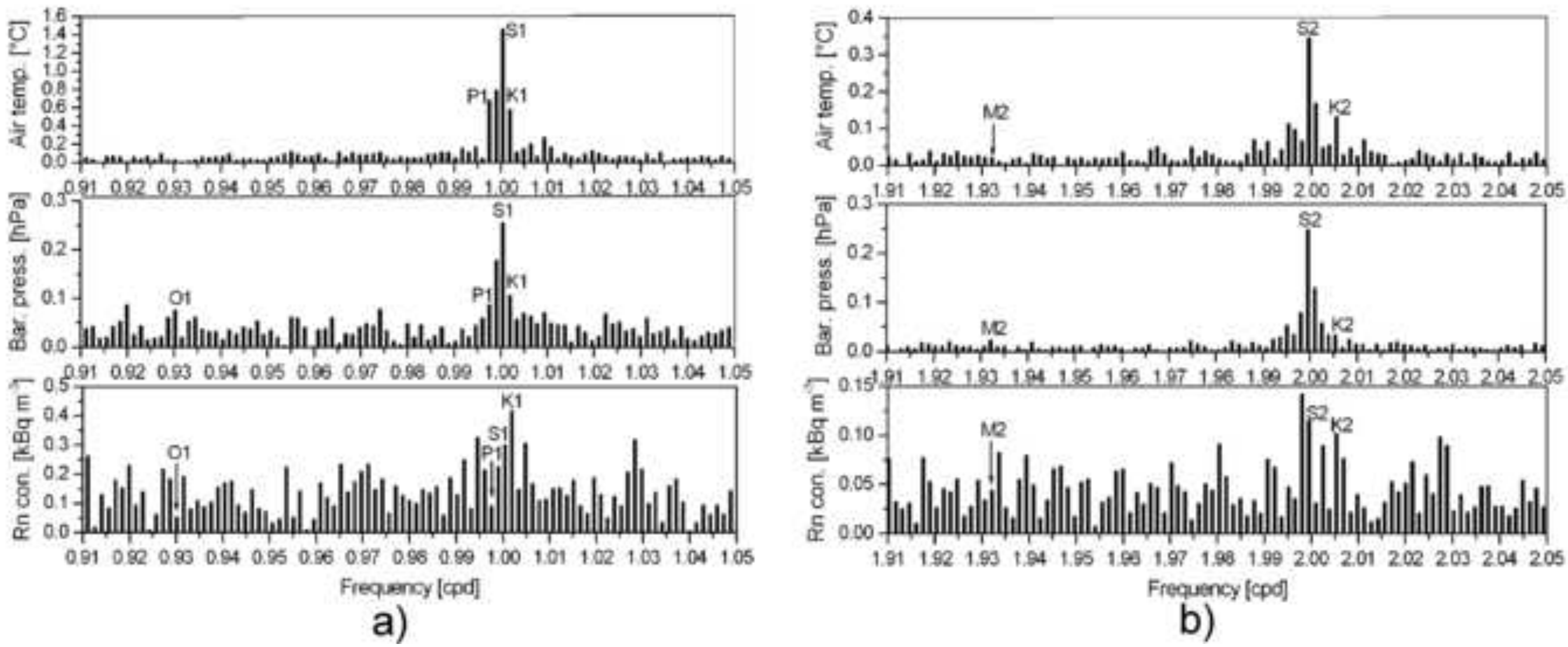

Figure 6
Click here to download high resolution image

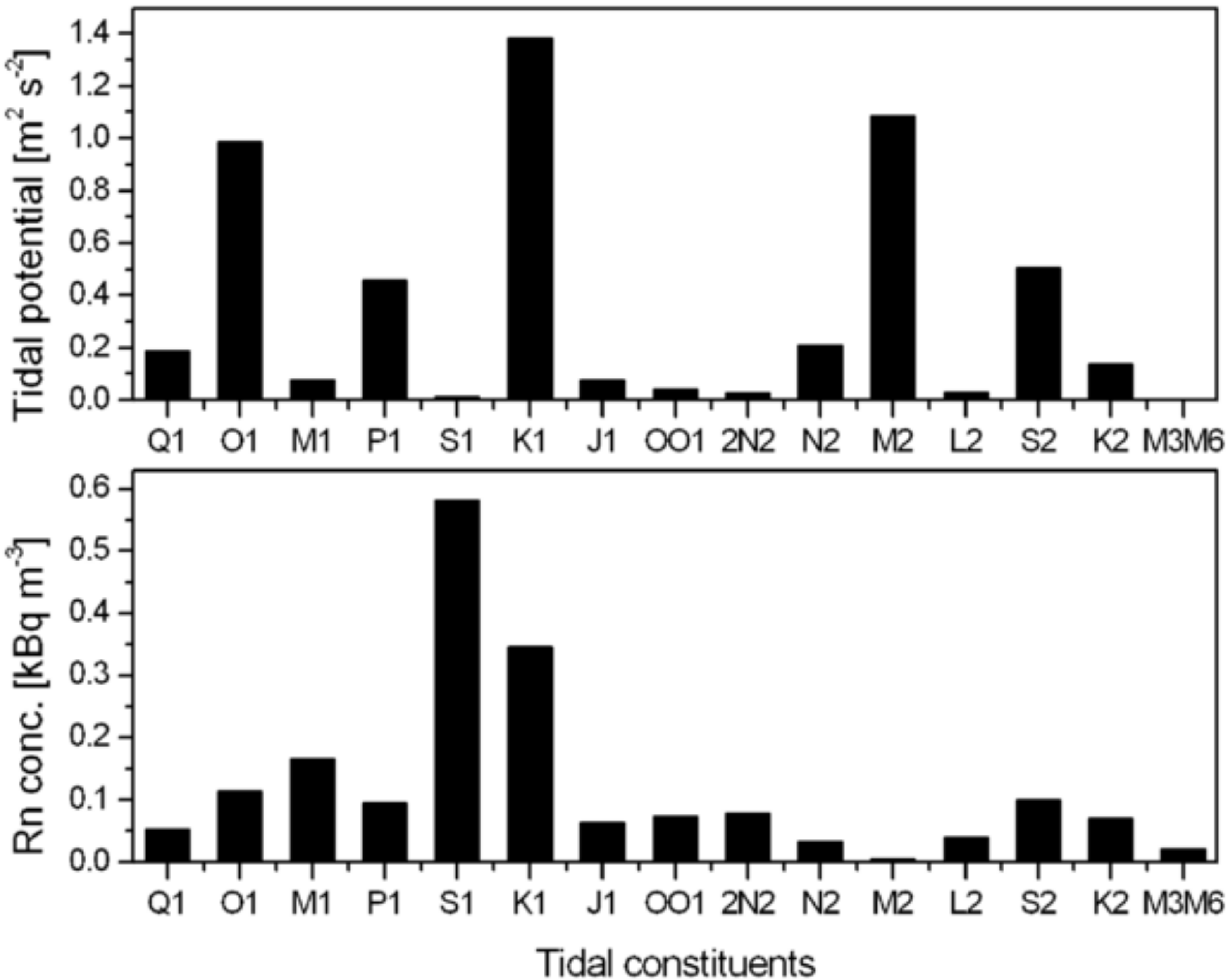

Figure 7

Click here to download high resolution image

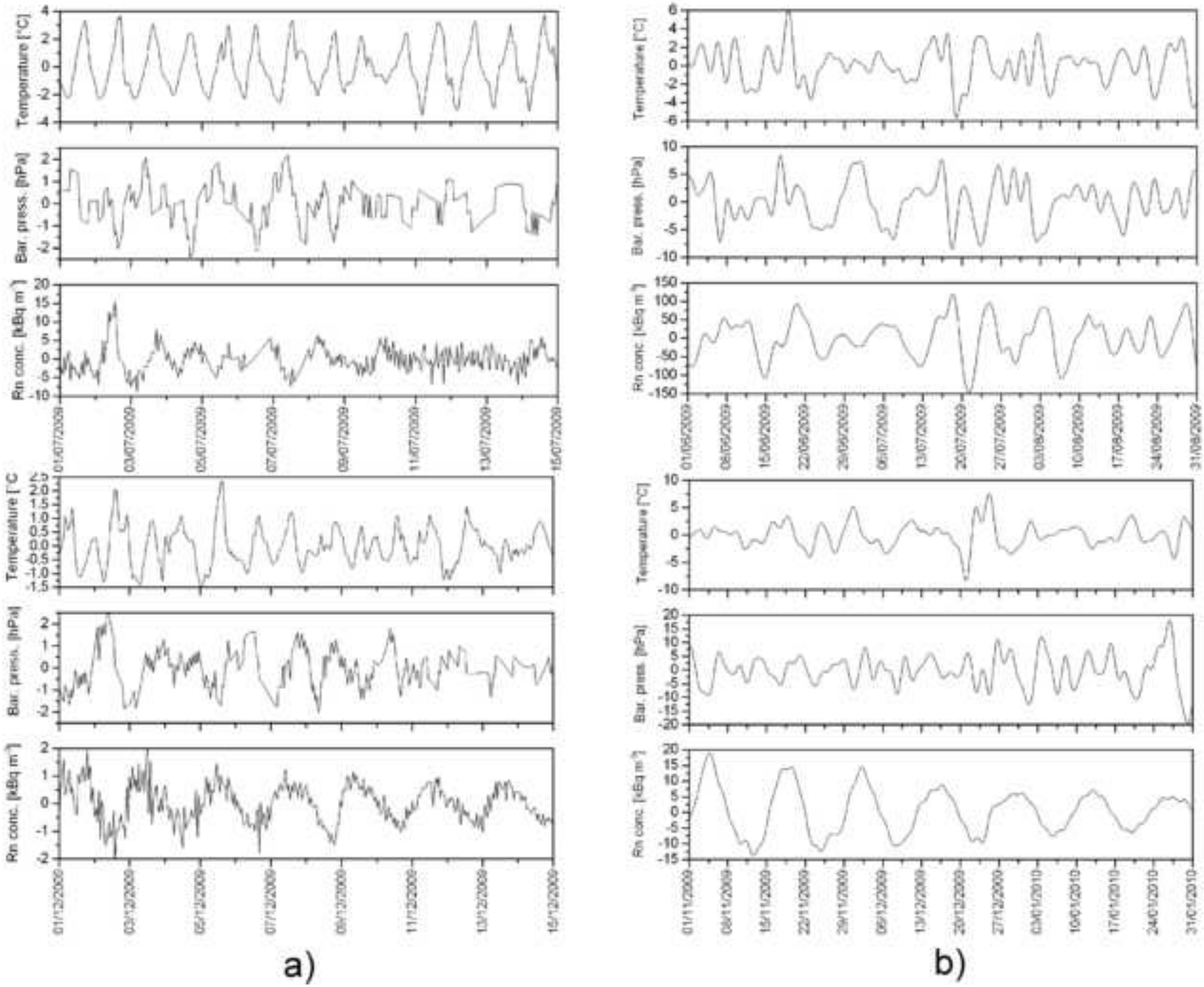

Figure 8
Click here to download high resolution image

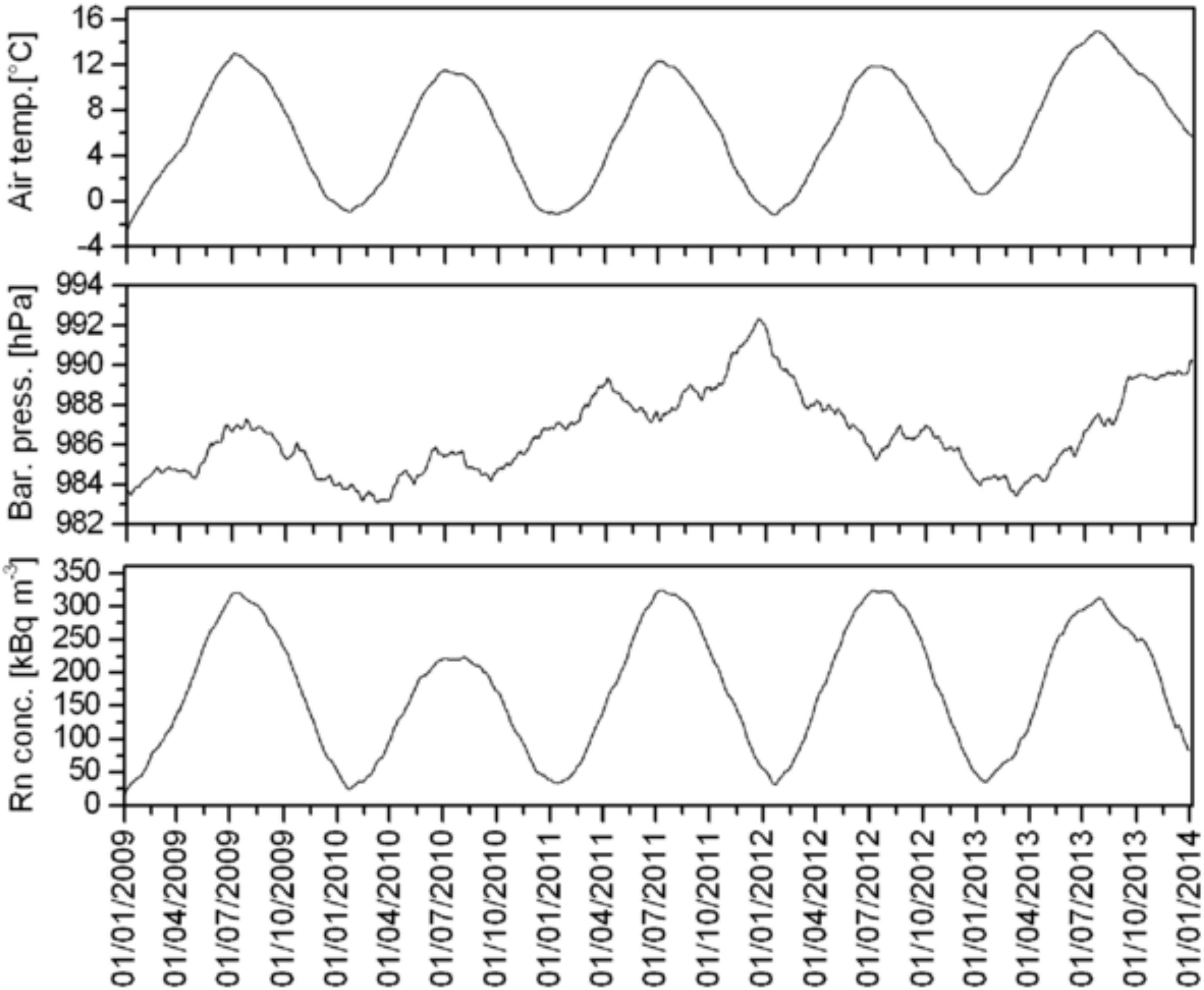

Table 1

Table 1. Results of correlation and regression analysis between Fourier amplitudes

Analysis method	Radon – temperature	Radon – bar. press.
Pearson correlation	0.70775	0.79932
Spearman correlation	0.36556	0.36722
Regression coefficients	16.982 kBq m^{-3} K^{-1}	9.8328 kBq m^{-3} hPa^{-1}

Table 2

Click here to download Table: Table-2.doc

Table 2. Results of the Principal Component Analysis

Time interval	Percentage of variability [%]		
	Radon concentration	Barometric pressure	Temperature
01.01.2009 – 31.12.2013	59.95	33.27	6.78
01.01.2009 – 31.12.2009	63.80	30.74	5.46
01.01.2010 – 31.12.2010	60.07	33.3	6.62
01.01.2011 – 31.12.2011	68.75	25.65	5.60
01.01.2012 – 31.12.2012	62.43	31.44	6.13
01.01.2013 – 31.12.2013	59.19	33.14	7.66
01.05.2009 – 30.09.2009	52.96	31.18	15.87
01.05.2010 – 30.09.2010	55.36	34.16	10.47
01.05.2011 – 30.09.2011	59.96	26.00	14.04
01.05.2012 – 30.09.2012	52.03	32.04	15.93
01.05.2013 – 30.09.2013	53.27	30.50	16.22
01.11.2009 – 31.03.2010	54.77	32.77	12.46
01.11.2010 – 31.03.2011	60.28	27.30	12.42
01.11.2011 – 31.03.2012	57.85	26.85	15.29
01.11.2012 – 31.03.2013	48.26	30.10	21.64

Table 3
Click here to download Table: Table-3.doc

Table 3. Results of the PLS analysis

Data type	Regression coefficients			
	Summer data		Winter data	
	Rn – T [kBq m^{-3} °C^{-1}]	Rn – P [kBq m^{-3} hPa^{-1}]	Rn – T [kBq m^{-3} °C^{-1}]	Rn – P [kBq m^{-3} hPa^{-1}]
Raw data	16.519	–2.315	1.064	–0.665
Daily average	25.936	–2.815	2.010	–0.635
Adjacent average	20.359	–1.458	21.597	5.298
Band–pass filtered	–1.313	–5.709	–0.750	–0.500
High–pass filtered	–0.233	0.206	–0.043	–0.112